Super Hydrophilic Semi-IPN Fluorescent Poly(N-(2-hydroxyethyl)acrylamide) Hydrogel for Ultrafast, Selective, and Long-Term Effective Mercury(II) Detection in a Bacteria-Laden System

Dong Zhang,[†] Yingchun Yao,[†] Jiahui Wu,[†] Iryna Protsak,[‡] Wei Lu,[*,§] Xiaomin He,[†] Shengwei Xiao,[‖] Mingqiang Zhong,[†] Tao Chen,[*,§,⊥] and Jintao Yang[*,†]

[†]College of Materials Science & Engineering, Zhejiang University of Technology, Hangzhou 310014, China

[‡]College of Environment, Zhejiang University of Technology, Hangzhou 310014, China

[§]Zhejiang Key Laboratory of Marine Materials and Protective Technologies, Ningbo Institute of Materials Technology and Engineering, Chinese Academy of Sciences, Ningbo, 315201, China

[‖]Department of Polymer Science and Engineering, School of Pharmaceutical and Chemical Engineering, Taizhou University, Jiaojiang 318000, Zhejiang, P. R. China

[⊥]University of Chinese Academy of Sciences, 19A Yuquan Road, Beijing 100049, China

S Supporting Information

ABSTRACT: Convenient, low-cost chemosensors for hazardous mercury ion detection have been receiving more and more attention in recent studies. However, most of these practical studies are based on an ideal sterile detecting atmosphere and ignore the role of bacteria in actual Hg(II) analytes. Herein, we demonstrate a new type of hydrophilic semi-IPN fluorescent polyHEAA hydrogel chemosensors fabricated by UV polymerization in situ interpenetrating fluorescent polymer PA-NDBCB with a polyHEAA network. Because of specific intermolecular interaction, i.e., hydrogen bonding between hydrophilic fluorescent polymer and polyHEAA matrix comprising a distinct semi-IPN structure, the mechanical property of bulk fluorescent hydrogels can be greatly improved over that of pure polyHEAA hydrogels. Moreover, the design of the hydrogel chemosensors rely on the highly efficient cyclization reaction between Hg(II) ions and the thiourea moieties that induce a visible "green-to-blue" fluorescence color change. On account of the hydrophilic porous structures, these hydrogel chemosensors achieve ultrafast, sensitive, selective Hg(II) detection (detection limit of 0.067 μM) and enable facile ratiometric actual detection in real-world aqueous system. Notably, they maintain fluorescence emission and detection property even under long-term coculture in a complex *E. coli* bacteria-laden environment. This novel strategy could inspire future construction of soft interfaces/fluorescent apparatus for hazardous Hg(II) detection in a complex real-world system.

KEYWORDS: semi-IPN, poly(N-(2-hydroxyethyl)acrylamide) hydrogel, mercury(II) detection, bacteria laden
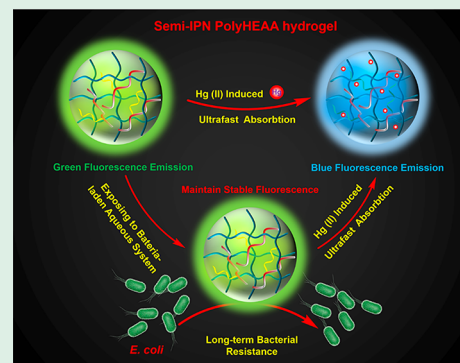
INTRODUCTION

Mercury ion pollution is a significant environmental issue affecting millions of people all over the world.[1,2] According to recent reports, Hg(II) ion accumulates in the vital tissues and animals organs, which can cause a variety of diseases.[3−5] Actually, Hg(II) ion entering the body through various means not only hinders the normal metabolism of cells but also causes neurotoxicity and renal toxicity-based multisystem damage of human body. Therefore, seeking effective methods for visual or real-time detection of mercury ions is becoming much more important.[6−9] However, most of these studies are primarily based on solution phases. In addition, actual analytes are always involved in the bacterial environment, such as polluted marine organism, plants, and water samples, yet few studies hae discussed the influence of bacteria under the pragmatic mercury(II) detection process.

Recently, solid-state fluorescent sensing materials have been gaining increasing attention and are being developed by facile operation.[10−13] For instance, Kim et al. have taken advantage of special design for recyclable polymeric film material, which allowed consecutive colorimetric highly selective mercury ions detection.[14] Yang and co-workers have originally combined pentiptycene-derived polymer with conjugated polymer backbones to prepare fluorescent film sensory materials which
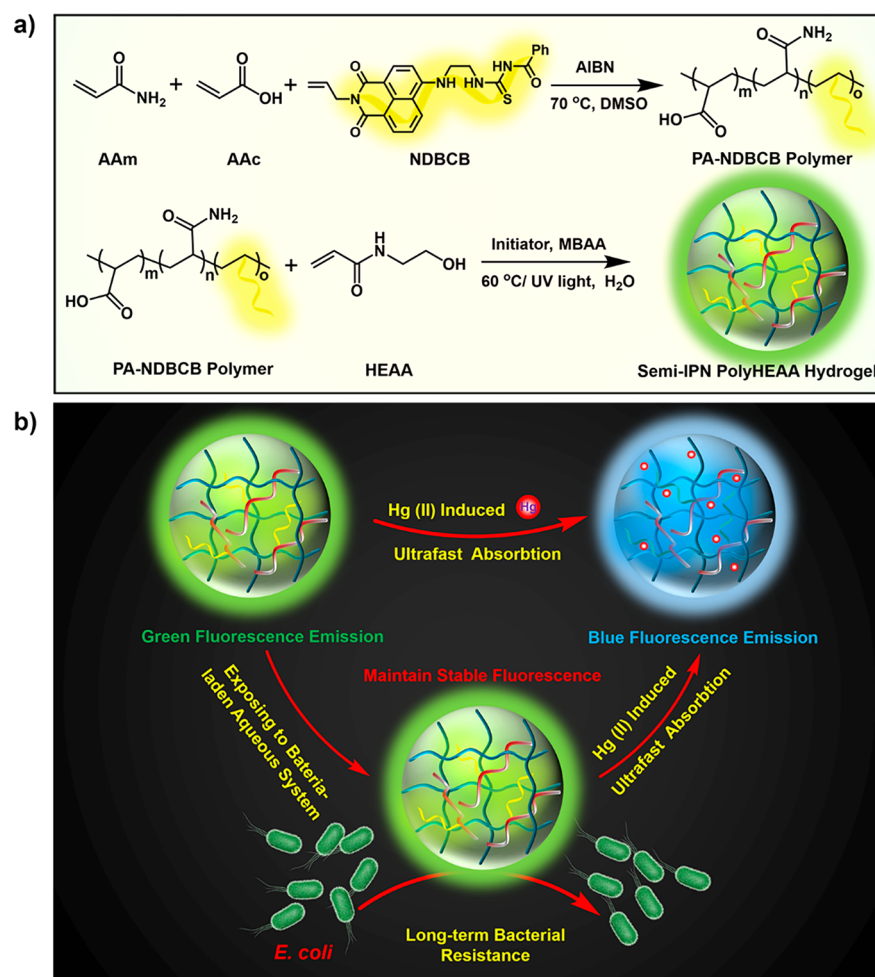
Figure 1. (a) Fabrication of fluorescent polymer PA-NDBCB and semi-IPN polyHEAA hydrogel chemosensors. (b) Long-term detection mechanism of semi-IPN polyHEAA hydrogel chemosensors in bacteria-laden system. As-prepared hydrogel emits green fluorescence upon exposure to aqueous Hg(II) solutions, Remarkably, after long-term coculture with *E. coli*, it still maintains stable fluorescence emission and mercury ion detection property as well, which is quite discrepant from the polyHEA hydrogel matrix. The excitation wavelength for all the fluorescence spectra is 365 nm.

exhibited larger response to nitro-aromatic compounds.[15,16] Furthermore, Lu et al. have presented a supramolecular cross-linked pyrene-functionalized fluorescent polymer film that realized the ultrafast detection for ultralow-level nitrobenzene pollutants.[17] All of these above-mentioned examples suggest that solid-state photoluminescent materials could become quite significant fluorescent sensing platforms for various hypertoxic pollutants.

The most challenging issue of these available advances is the restricted sensing procedure caused by blocked slow diffusion. Note that hydrogels consist of a large number of hydrophilic network structures that allow rapid pollutant absorption-identification, and can somehow be good candidates for ratiometric detection in aqueous system.[18−31] It is worth mentioning that our group recently presented a novel kind of hydrophilic fluorescent composite hydrogel chemosensor that achieved visual and ratiometric detection of nM-level mercury ions based on the specially designed NDBCB naphthylimide-derivative.[32] According to the previous studies for this green fluorescent naphthylimide-derivative NDBCB ((N-((2-((2-allyl-1, 3-dioxo-2, 3-dihydro-1H-benzo[de]isoquinolin-6-yl)-amino)-ethyl)-carbamothioyl)-benzamide)), a special cycliza-tion of designed thioureas leads to the formation of a high-

intensity blue fluorescence in the presence of Hg(II) ion, which is also adapted in electrospun nanofiber and paper film materials.[12,32,33,46] However, the lengthy detection time has limited their further rapid practical application. On the other hand, plenty of hydrogel-related chemosensors can be easily contaminated by impurity interference and bacterial/protein adhesion during the long-term aqueous detection process, which eventually give rise to device failure. Interestingly, some antifouling/self-cleaning materials can effectively solve these problems.[34,35] For instance, our group recently developed a novel hydrophilic polymer polyHEAA, which prevented the initial attachment of bacteria/protein on the substrate surface and allowed us to establish long-term antifouling behav-ior.[36−38] Imagine: if an antifouling/self-cleaning function can be assembled into the molecular meshes that are covered at the detecting surface of the hydrogels, the effective time of hydrogel chemosensors will be greatly promoted in complex environments.

Herein, a new type of hydrophilic semi-IPN fluorescent polyHEAA hydrogel chemosensors is presented that enables ultrafast sensitive, selective, and long-term effective mercury-(II) detection in aqueous solutions. These semi-IPN hydro-philic hydrogels are fabricated by UV radical polymerization of
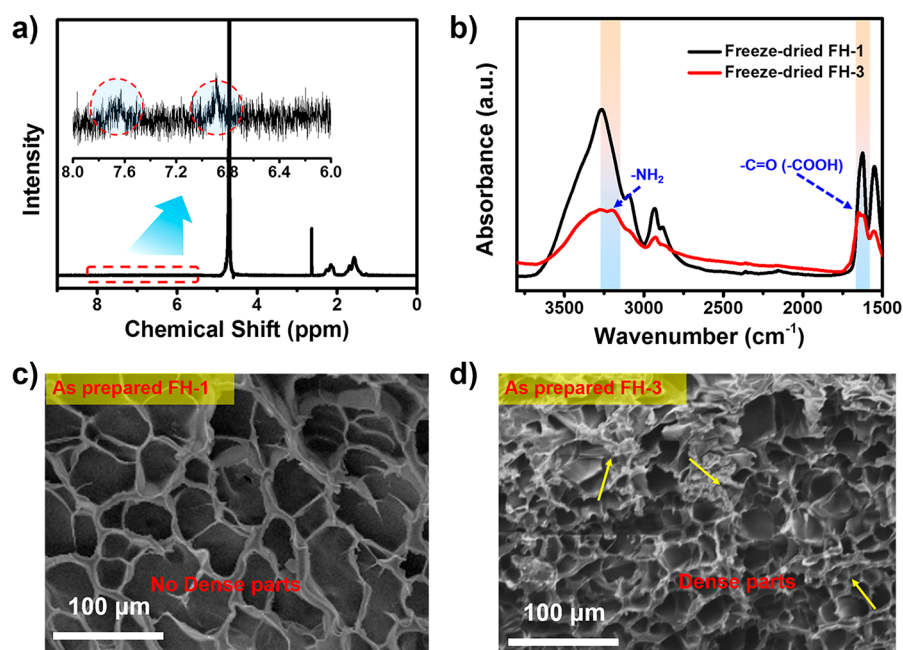
Figure 2. Chemical structure and morphology of semi-IPN hydrogels FH-3 and pristine hydrogel FH-1. (a) ^{1}H NMR spectrum of PA-NDBCB in DMSO-d_6; (b) comparison of ATR-FTIR spectra of free-dried FH-1 and FH-3 hydrogels; (c, d) SEM images of as-prepared FH-1 and FH-3 hydrogels (fully freeze-dried).

N-(2-hydroxyethyl)acrylamide, I-2959 initiator and MBAA cross-linker in situ-interpenetrating as-designed fluorescent hydrophilic copolymer PA-NDBCB (Figure 1a). Obviously, the pristine hydrogels emit green fluorescence when exposed to Hg(II) aqueous solution and the fast positive driving force from hydrophilic porous structures induces rapid contact between Hg(II) ion and special thiourea groups, which eventually induce desulfurization/cyclization reaction to produce blue luminescence guanidine derivatives (Figure 1b and Figure S1). Therefore, these hydrogel chemosensors generate ratiometric and visual color change (The detection limit reaches 0.067 μM). Remarkably, due to the as-constructed semi-IPN structures and strong hydrogen bond interaction, the hydrogel chemosensors effectively improve their mechanical properties, including tensile strength and breaking elongation, as compared with noninterpenetrating hydrogels. The most significant point is that our semi-IPN fluorescent polyHEAA hydrogels maintain stable fluorescence emission and detection properties even with the long-term coculture in *E. coli* bacteria-laden environment. This work provides a novel strategy and holds a great potential in the construction of soft sensing apparatus for hazardous mercury detection in real-world systems.

■ EXPERIMENTAL SECTION

Materials. Acrylamide (AAm), N, N′-methylenebis(acrylamide) (MBAA), acrylic acid (AAc) and ethyl alcohol were used as received from Aladdin Co., Ltd. AIBN, dimethyl sulfoxide (DMSO), potassium persulfate (KPS), 2-hydroxy-4′-(2-hydroxyethoxy)-2-methylpropiophenone (I-2959), 2-hydroxyethyl acrylate (HEA) and N-(2-hydroxyethyl)acrylamide (HEAA) were purchased from J&K Scientific Co., Ltd. All metallic nitrates of metal ions (including Hg^{2+}, K^+, Mg^{2+}, Al^{3+}, Ag^+, Fe^{2+}, Cr^{2+}, Ni^{2+}, Cd^{2+}, Pb^{2+}, Fe^{3+}, Zn^{2+}, and Pt^{2+} ion) were purchased from Sigma-Aldrich Co., Ltd. All other reagents were used as received. NDBCB ((N-((2-((2-allyl-1, 3-dioxo-2, 3-dihydro-1H-benzo[de]isoquinolin-6-yl)-amino)-ethyl)-carbamo-

thioyl)-benzamide)) was used as a fluorescent monomer and was synthesized according to our previous research.[32]

Synthesis of Fluorescent PA-NDBCB Copolymer. PA-NDBCB was prepared by the common radical copolymerization method. The mixture containing AIBN (20 mg), acrylic acid (1.70 g), acrylamide (0.30 g), NDBCB (5 mg), and DMSO (12 mL) was poured into a polymerization pipe. After degassed by N_2 flow 3−6 times (10 min), the pipe was placed at 70 °C for 8 h. Later, the reaction solution changed to a highly viscous liquid, the product was further precipitated by ethyl alcohol and purified by two-day DI water dialysis processing and then dried for use. The dried hydrophilic fluorescent copolymer PA-NDBCB was redissolved in DI water with 3, 6, and 10 wt % concentration, respectively, for standby.

Preparation of Semi-IPN Fluorescent Hydrogels. In our as-designed system, there are two different methods for the preparation of fluorescent hydrogels: thermal and UV copolymerization (Table S1). Mixtures containing 1.5 mL of fluorescent copolymer aqueous solution (with different concentrations, from 0 to 10%), HEAA (2.0 g), MBAA (3 mg) and initiator KPS or I-2959 (20 mg) were all poured into a 20 mL beaker to dissolve the reagents sufficiently. After being degassed by N_2 flow three times (10 min), the well-dispersed solution was injected into the prefabricated glass-mold spacer with a 1 mm silicone sheet. Photopolymerized semi-IPN hydrogels (FH-1 ∼ FH-4) were then fabricated under 365 nm UV irradiation (1 h); or the glass spacer was heated up to 60 °C for 10 h by thermal-polymerized hydrogels preparation (FH-5 ∼ FH-8). In addition, the semi-IPN polyHEA hydrogel (FH-9) was also obtained by the above-mentioned photopolymerization method.

Chemical Structure by ^{1}H NMR. ^{1}H NMR spectrum of PA-NDBCB copolymer was recorded on Bruker Avance AMX-400 Spectrometer by DMSO-d_6.

FTIR-ATR Measurement. FTIR-ATR spectra were recorded on the Micro FT-IR (Cary660 + 620; the resolution is 4 cm^{-1}). The hydrogel samples contain both fluorescent copolymer and freeze-dried hydrogels.

Morphology Characterization by Scanning Electron Microscope. The morphology of fluorescent hydrogels (freeze-dried) were measured by scanning electron microscopy equipped with an energy dispersive spectrometer detector.
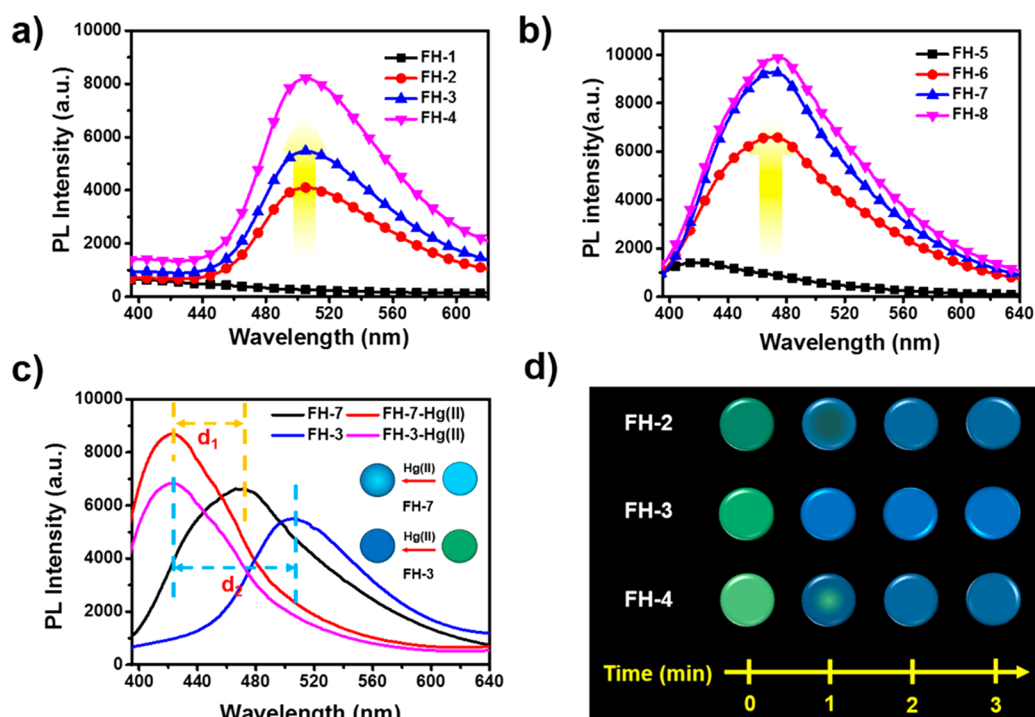
Figure 3. (a, b) Typical fluorescence spectra of the semi-IPN polyHEAA hydrogels with different amounts of PA-NDBCB polymer for both UV polymerization (FH-1–FH-4) and thermal polymerization (FH-5–FH-8). (c) Comparison of fluorescence spectra between UV- and thermal-polymerization polyHEAA hydrogel (FH-3 and FH-7) before and after being immersed in aqueous Hg(II) solutions (1×10^{-5} M). Note that d_1 and d_2 belong to the blue-shifted displacements in detection processes for FH-7 and FH-3 hydrogels. (d) Photographs showing the time-dependent emission color change with treatment of 1×10^{-5} M Hg(II) ion solution for FH-2, FH-3, and FH-4, respectively. Here, all hydrogel samples were cut into disc shape (diameter of 1 cm and thickness of 1 mm) by a laser cutter. The excitation wavelength for all the fluorescence spectra is 365 nm.

Fluorescence Property Measurement. The fluorescence spectra of fluorescent copolymers, aqueous solutions and hydrogels were measured by Hitachi F-4600 spectrofluorometer (150 W xenon lamp; 365 nm UV). Before testing fluorescent properties, full UV irradiation were treated on the hydrogel samples both in the presence and absence of bacteria to ensure the safety of the operator.

Mechanical Characterization. The rheological properties of as-prepared fluorescent hydrogels (both FH-1 and FH-3, disc-shaped, and 1 mm thickness) were measured using a Physica MCR-301 rheometer (Andongpa Co. Lt., Austria) at room temperature. Tensile measurements of as-prepared and equilibrated fluorescent hydrogels (both FH-1 and FH-3) were measured by the commercial tensile tester (Instron Co. Lt.). Specifically, the hydrogels were sliced into dumbbell shape (12 mm length L_0 and 2 mm width). Here, the rate of extension is controlled for 100 mm/min.[39]

Long-Term Bacteria Coculture. *Escherichia coli* was applied as a model bacteria, and was incubated at 37 °C in Luria–Bertani (Agar plates). After the bacteria were incubated in a shaking incubator, the cultures were diluted to controlled condition (0.1 value under 600 nm UV). After 10 min UV sterilization, all hydrogels also were incubated at 37 °C for 0–48 h.[37,40,41] The both polyHEAA and polyHEA hydrogels were removed and treated with LIVE/DEAD BacLight Kit for fluorescent recognition. After about 10 min dyeing, all hydrogel samples were observed directly by utilizing a fluorescence microscope with a 40× lens.

■ RESULTS AND DISCUSSION

Preparation of Semi-IPN Fluorescent Hydrogels. The fluorescent NDBCB monomer was prepared by our previous research,[32] after that, fluorescent copolymer PA-NDBCB was fabricated through a simple radical copolymerization (Figure 1 and Figure S1) and purified. Thereafter, the obtained copolymer was analyzed by ^{1}H NMR (Figure 2a). From the ^{1}H NMR of PA-NDBCB copolymer, a distinct aromatic proton

signals appeared in expanded region. The yield of NDBCB in this copolymerization is nearly 56%. Although the NDBCB monomer was basically hydrophobic, the PA-NDBCB copolymer exhibited high hydrophilicity due to the high mass ratio of extremely hydrophilic comonomers acrylamide and acrylic acid (The water contact angle is 76.4° in Figure S2). Accordingly, PA-NDBCB copolymer could be easily dissolved in water, showing a viscous aqueous solution which emits yellowish-green fluorescence (Some other characterizations of PA-NDBCB copolymer, such as DSC, ATR spectra, were also provided in Figure S3–S4).

By using the PA-NDBCB copolymer, Semi-IPN fluorescent hydrogels were then prepared through the synthetic procedures (see Figure 1) according to various feed ratios mentioned in Table S1 (From 0 wt % ~ 10 wt %), which were termed as FH-1 ~ FH-9 hydrogels. When compared the SEM images of as-prepared FH-1 with FH-3 (Figure 2c, d), some dense parts with compact pores can be observed in Figure 2d, which is likely induced by the presence of the copolymers. FTIR-ATR spectra of as-prepared FH-1 and FH-3 hydrogels were further characterized as shown in Figure 2b. Two peaks that locate at ~1700 cm^{-1} and ~3200 cm^{-1} corresponding to the −C=O (−C(=O)OH) stretching and −NH$_2$ bending vibration can be observed, respectively, indicating the existence of the copolymers. The semi-IPN network structure could be clearly distinguished by the combination of SEM and FTIR-ATR results.

Effect of Polymerization Processes on Semi-IPN Fluorescent Hydrogels. According to our previous study,[32] PA-NDBCB possessed excellent Hg(II)-induced responsive property. Because of the existence of naphthalimides group,
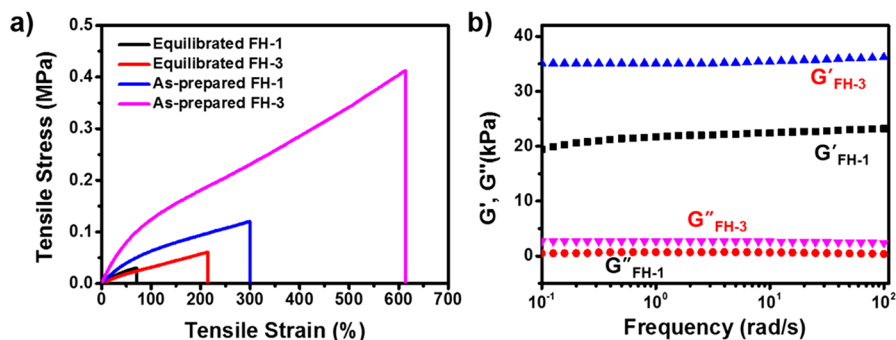
Figure 4. Mechanical properties of semi-IPN polyHEAA hydrogel (FH-3) and pristine polyHEAA hydrogels without semi-IPN structure (FH-1). (a) Tensile curves (stress−strain) of as-prepared/equilibrated FH-1 and FH-3 hydrogels; (b) frequency dependence of the G' and G'' of the as-prepared FH-1 and FH-3 hydrogels (disc shape).
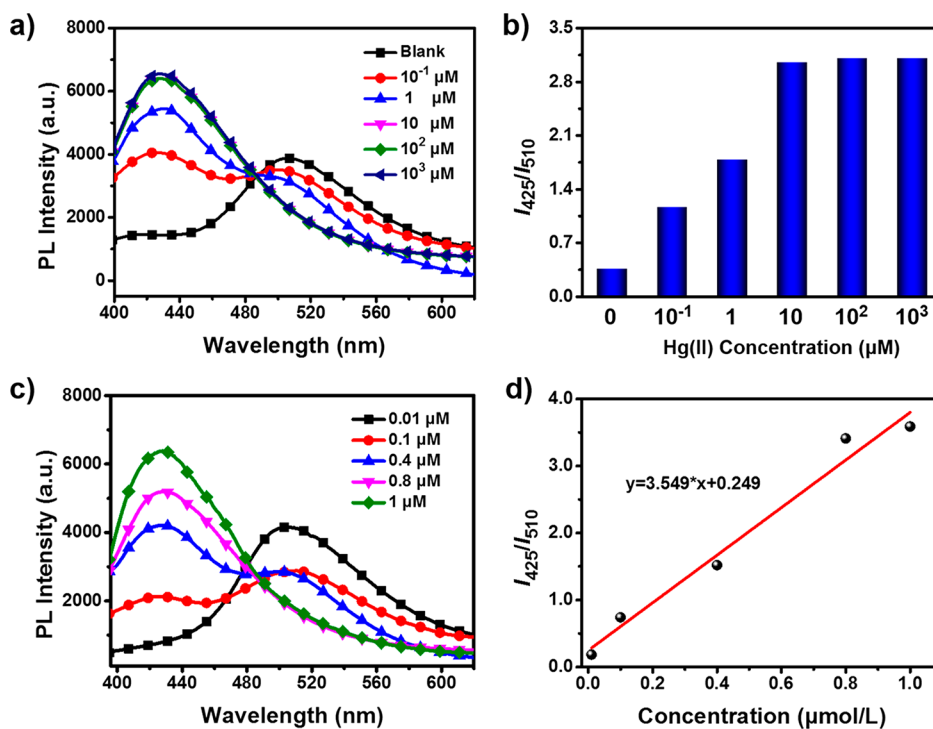

Figure 5. (a, c) Mercury-concentration-dependent fluorescence spectra of the semi-IPN polyHEAA hydrogel chemosensors (FH-3) (0.01 μM to 1 × 10³ μM). (b) Emission intensity ratio I_{425}/I_{510} of FH-3 hydrogels with which were treated in various Hg(II) ion concentration solution ("blue" at 425 nm and "green" at 510 nm); (d) Fluorescent ratiometric linear fitting for intensity ratio I_{425}/I_{510} of FH-3 hydrogels in the range of 0.01−1 μM Hg(II) aqueous solution. The excitation wavelength for all the fluorescence spectra is 365 nm.

the copolymer exhibited fluorescence emission at 510 nm, whereas when it is exposed to mercury ion aqueous solutions, the special desulfurization of the thiourea groups from PA-NDBCB immediately occurred and the corresponding blue fluorescence derivatives were produced by the promptly following cyclization. As a result, the fluorescent emission was blue-shifted to 425 nm. Thus, PA-NDBCB was designed into polyHEAA network by semi-IPN structure to create mercury ion hydrogel chemosensor. Herein, two methods, i.e., thermal-initiated and UV-initiated polymerizations, were used for the preparation of the hydrogels. It is interesting to observe that the polymerization type exhibited a significant influence on the fluorescence emission performance of the semi-IPN hydrogels. Figure 3a, b shows the fluorescence spectra of hydrogels from different polymerizations (FH-1−FH-4 and FH-5−FH-8 from UV and thermal initiated polymerizations, respectively). It can be seen that FH-1−FH-4 emitted green

fluorescence (λ_{max} = 510 nm) with varied intensities depending on the concentration of the PA-NDBCB, whereas FH-5−FH-8 hydrogels showing a conspicuous blue shift and emitting blue-green fluorescence (λ_{max} = 470 nm). We speculate this phenomenon derives from the famous Wien displacement law,[42] because the blue-shift rate will vary because of the difference in the amount of heat/temperature given. As is known, the temperature of thermo-polymerization must be greater than 60 °C, whereas the photopolymerization always initiated at room temperature. Therefore, during the polymerization process, some arresting electron transfer (blue shift) phenomena were easily generated, especially for the thermo-polymerization. The corresponding images of laser-cut practical samples also exhibited similar difference in fluorescence emission between UV- and thermally initiated polymerizations.
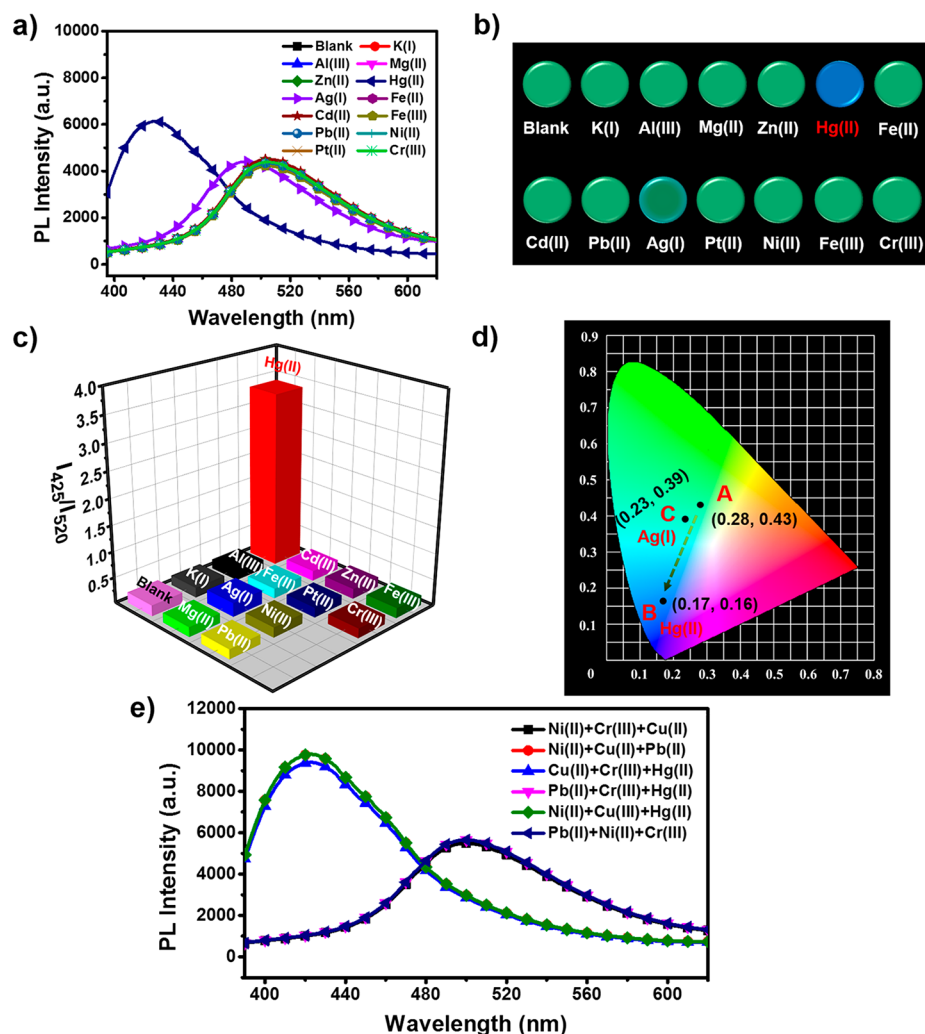
Figure 6. (a) Fluorescence spectra of the semi-IPN polyHEAA hydrogel chemosensors (FH-3) of various hazardous metal ions; (b) Photographs of the FH-3 hydrogels, which were taken under a hand-held UV lamp at 365 nm excitation (treated with 1×10^{-5} M solutions of various metal ions). (c) I_{425}/I_{510} values of the FH-3 hydrogels in response to various metal ions. Similarly, all hydrogel samples were cut into disc shape (diameter of 1 cm and thickness of 1 mm) by a laser cutter; (d) CIE coordinates transition (before/after exposure to polluted solution at 365 nm excitation). For point C, it belongs to the Ag (I) treatment group, which shows a slight blue shift; (e) Anti-interference property of Hg(II) detection of FH-3 hydrogel.

The influence of the polymerization method on mercury stimuli-responsive for hydrogel was further investigated. In Figure 3c, regardless of any copolymerization approaches taken, all the obtained hydrogels display accordant Hg(II) stimuli response and the fluorescence-emission peaks blue-shifted to 425 nm. However, when compared the changes in the fluorescence-emission caused by the presence of Hg(II) as indicated by d_1 and d_2, we can see that the hydrogel from UV polymerization method seems to possess a larger blue shift displacement, demonstrating that it is easier to distinguish the detection results than that from thermal polymerization. Such larger peak displacement, actually was also beneficial to the whole visual and real-time Hg(II) detection process. Figure 3d depicts the fluorescence-emission images of the FH-2−FH-4 hydrogels exposed to 1×10^{-5} M Hg(II) solutions for different time. It is clear that the conspicuous fluorescence transition has been observed in several minutes for all the prepared hydrogels. This color change rate is much faster than that of hydrogel-coated paper/textile chemosensors in our previous study,[32] likely due to the high hydrophilicity of polyHEAA which induces the fast permeation of solution with Hg(II).

The color change rate also showed a copolymer concentration dependence, where FH-3 showed the fastest rate among these hydrogels, showing the potential to create ultrafast detection efficiency. Therefore, in order to obtain the optimal fluorescent hydrogel chemosensor, we need to regulate the amount of semi-IPN polymer in hydrogel matrix precisely.

Favorable Mechanical Properties of Semi-IPN Hydrogels. Inspired by plenty of researches of semi-IPN hydrogels,[43−45] the mechanical properties of our semi-IPN polyHEAA hydrogel could be enhanced effectively. Here, the linear PA-NDBCB copolymers were interpenetrated within as-designed polyHEAA hydrogel matrix by hydrogen-bond interaction. Both as-prepared and equilibrated semi-IPN hydrogels (FH-3) showed better mechanical performances, higher elastic than FH-1 hydrogels with the similar state (Figure 4a). Becauseof the formation of more compact networks, semi-IPN structure effectively enhanced the mechanical properties to polyHEAA matrix (the breaking stress (σ_b) and strain (ε_b) increased ~4 times and ~2 times, respectively). The storage modulus G' and the loss modulus G'' of both as-prepared FH-1 and FH-3 were further
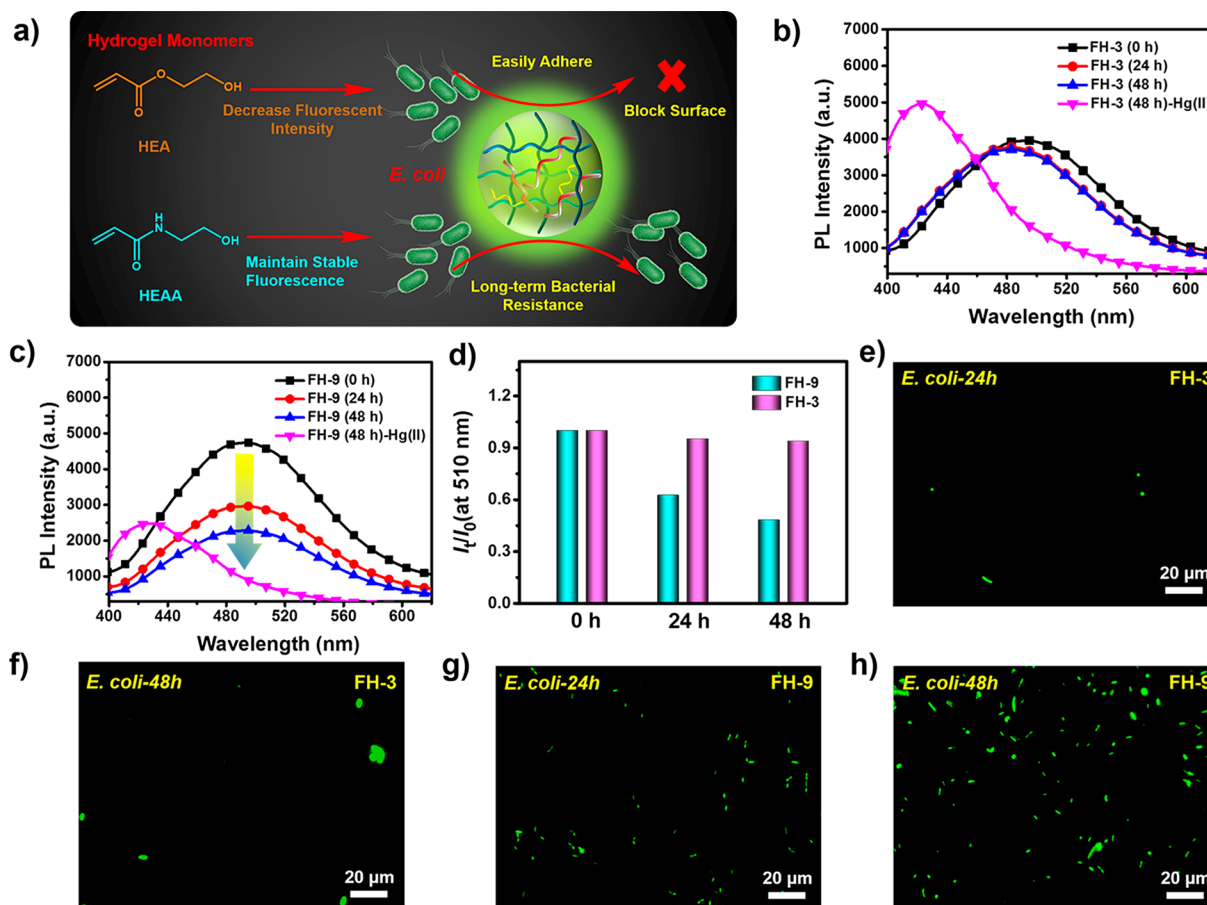
Figure 7. Effects of hydrogel matrix on the fluorescence properties. (a) Mechanism of two hydrogel matrixes on the fluorescence emission process, which derived from HEAA and HEA monomers. Here, semi-IPN polyHEAA fluorescent hydrogels maintain their fluorescence emission because of their superb nonfouling performance, whereas polyHEA hydrogels make the bacteria adhere onto the surface easily and finally block the surface due to their unsatisfactory antifouling property; (b, c) Time-dependent change of fluorescence spectra between FH-3 and FH-9 hydrogels for *E. coli* coculture; (d) emission intensity ratio I_{425}/I_{510} of FH-3 and FH-9 hydrogels for 0−48 h *E. coli* coculture; (e, h) fluorescence images of *E. coli* for FH-3 and FH-9 hydrogels (both 24 and 48 h). The excitation wavelength for all the fluorescence spectra is 365 nm.

investigated by oscillatory rheometer (Figure 4b). The quantitative value of G' of the FH-3 hydrogel was much even greater than the FH-1 hydrogel, which also indicated effective enhancement for regulation of semi-IPN structure.

Sensitivity and Selectivity of Mercury(II) Detection. For semi-IPN hydrogel of polyHEAA and PA-NDBCB, a very fast fluorescent color change has been observed. Some other properties, such as sensitivity and selectivity, are equally or even more important for sensing materials. Thus, the semi-IPN hydrogel was exposed to solutions with various concentration of mercury ions, and the fluorescent emission spectra were recorded. Here, the adopted concentration of Hg(II) ion ranged from 1×10^{-3} M to 10^{-7} M, and the FH-3 hydrogel was exposed to the solution for 2 min. As shown in Figure 5a, without Hg(II), the hydrogel showed fluorescent emission at 510 nm, while in the presence of Hg(II), it can been seen that at a very low concentration (10^{-7} M), the fluorescent emission at 425 nm appeared, albeit the fluorescent emission at 510 nm still existed. When the concentration was higher than 1×10^{-5} M, only the emission peak at 425 nm could be obviously observed in the spectra. The intensity ratio between the emissions at 425 and 510 nm (e.g., I_{425}/I_{510}) was used as an indicator to further depicting the mercury responsive behavior (Figure 5b). The change of I_{425}/I_{510} showed similar trend with that of the emission spectra. For pure water, I_{425}/I_{510} of the

hydrogel was as low as 0.35, and greatly increased to ~1.2 when 1×10^{-7} M Hg(II) ions existed. The great change in I_{425}/I_{510} of the hydrogel from water to solution with 1×10^{-7} M Hg(II) ion indicated that this hydrogel was applicable for testing the existence of Hg(II) with such low concentration. Further increasing the normal concentration of mercury ion (1×10^{-6} M and 1×10^{-5} M), the I_{425}/I_{510} gradually increased to ~1.8 and ~2.8. When the Hg(II) ion concentration was higher than 1×10^{-5} M, the I_{425}/I_{510} kept constant at ~2.8. These results suggested that as-designed semi-IPN fluorescent hydrogel could work even as a ratiometric chemosensor. Because this ratiometric chemosensor provided the build-in relationship between 425 and 510 nm emission peaks for ambient stimuli, thus they holding potential to precisely quantify the Hg(II) concentration in complex real-world aqueous sample. Remarkably, the developed fluorescent hydrogel is so sensitive to detect Hg(II) ion, even lower than 1×10^{-7} M.

To determine the exact detection limit of the hydrogel, we prolonged the exposure time to 15 min to further enlarge the I_{425}/I_{510} value. Five concentrations of mercury ion (0.01 to 1 μM) were used, where the I_{425}/I_{510} exhibited a good linear relationship to the concentration (Figure 5c, d). On the basis of linearly fitting the relation between I_{425}/I_{510} and Hg(II) ion concentration, the detection limit was calculated as 0.067 μM

by the followed formula (eq 1) from the according method.[46] Compared to previous research[4,7,32,47,48] (Table S2), the detection limit of this fluorescent semi-IPN hydrogel is slightly higher, likely due to plenty of pre-existing water in the hydrogel, which plays a dilution role in the hydrogel.

$$\text{detection limit} = 3\sigma/\text{slope} = 3\cdot0.08/3.549 = 0.0676$$

$$\mu M; \;\; \sigma = 0.08; \;\; \text{slope } (K) = 3.549 \tag{1}$$

In reality, Hg(II) ions are always accompanied by many other different ions which sometimes significantly interfere response behavior of the chemosensor.[33] To investigate the sensing selectivity of our hydrogel toward Hg(II) ion, the emission transitions with more common ions were further studied (Figure 6).

As classified in Figure 6a−c, no fluorescence transition was observed for most of the tested metal ions. It was noted that Ag^+ ion was able to form a blue-shift of the emission band; however, its intensity variation is not particular distinct. Furthermore, the evidence for excellent selectivity behavior of our semi-IPN hydrogel came from the visual detection photographs (Figure 6b). For better displaying this visual detection process, the CIE coordinate was provided in Figure 6d; they changed from (0.28, 0.43) to (0.17, 0.16). In addition, the anti-interference property of Hg(II) detection of FH-3 hydrogel was also provided by adding other disruptive heavy metal ions (Cu^{2+} and Pb^{2+}), showing its outstanding Hg(II) selectivity in more complex aqueous solution (see Figure S6). Figure 6e further provided fluorescence spectra change for hydrogel chemosensor by tolerating with various heavy metal ion composite solutions (including Ni^{2+}, Cu^{2+}, Pb^{2+}, Cr^{3+}, and Hg^{2+}). Obviously, this kind of soft chemosensor reveals special anti-interference (selectivity) behavior for mercury ion detection.

Long-Term Mercury(II) Detection in Bacteria-Laden System. For the real-word application of sensors for Hg(II) detection, industrial wastewater with many organic pollutants is one of most common environments. Therefore, antifouling properties become of critical importance because it plays the key role in dictating the long-term behavior. To test its longstanding detection property in wastewater, bacterial solution was used as a model solution to challenge the hydrogel, and the Hg(II) responsive behavior after different treating time was measured. For comparison, similar semi-IPN hydrogel (FH-9) based on polyHEA that is one of most commonly used polymer in biological community was also tested. As shown in Figure 7b−d, upon nearly 48 h coculture to *E. coli*, FH-3 hydrogel produced very stable fluorescence emission while the fluorescence intensity of FH-9 hydrogel dropped dramatically. However, these two hydrogels still had the ability to detect mercury ions. We speculated that these results mainly came from the monomer or hydrogel matrix of semi-IPN system. Note that polyHEAA material, as our previous studies shown,[36,37] was an excellent antifouling material that can withstand nearly 4 weeks of bacterial culture. Therefore, semi-IPN polyHEAA fluorescent hydrogel can maintain the competence of fluorescence emission well. However, it was easier for bacteria to adhere onto polyHEA surface due to unsatisfactory antifouling property, which induced the energy transfer process and eventually blocked the fluorescence emission (Figure 7a). Remarkably, the images of *E. coli* for both FH-3 and FH-9 hydrogels (24h and 48 h) were also provided in Figure 7e−h. Moreover, the swelling

processes of polyHEAA and polyHEA hydrogels in DI-water were also provided (Figure S5), which ruled out possibility of the effect of swelling coefficient on fluorescence performance. Considering these semi-IPN polyHEAA hydrogels can even tolerate bacteria-laden environment, we believe that these hydrogel chemosensors will have great application potential in complex real-world system, especially for the soft intelligent detection actuator.

Application of Semi-IPN PolyHEAA Hydrogels. It is of great important for applying sensing devices to actual aqueous system. Hence, the detection performance of mercury ion in complex aqueous samples were further determined (Figure 8).
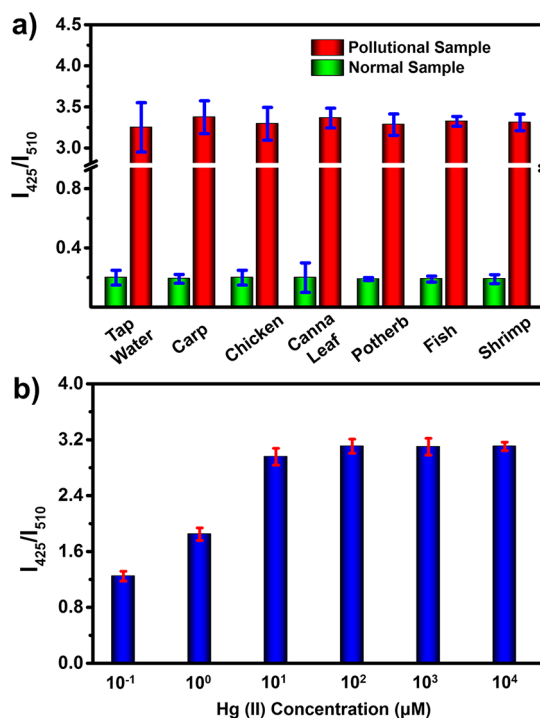

Figure 8. (a) Hydrogel chemosensor application for detection of real-world water and food samples. Emission intensity ratio I_{425}/I_{510} values of FH-3 semi-IPN polyHEAA hydrogel in response to some nonpolluting and polluted practical samples at 365 nm excitation, including tap water, carp, chicken, fish, potherb, canna leaf and shrimp samples. (b) Emission intensity ratio I_{425}/I_{510} of FH-3 hydrogels with which were treated in various Hg(II) ion concentration aqueous solution samples ("blue" at 425 nm and "green" at 510 nm).

Seven water/food samples (chicken, canna leaf, potherb, fish, tap water, shrimp and carp) were selected as representative examples. Tap water was filtered before measuring, while other samples were prepared into solutions according to the solvent extraction processes with HNO_3/H_2O_2 mixed solution. In Figure 8a, the results revealed a commendable consistency and demonstrated the weeny effect for real-world samples, suggesting the prepared semi-IPN polyHEAA hydrogel could be an excellent ratiometric chemosensor candidate for practical applications. Moreover, the correlation between fluorescence intensity ratio (I_{425}/I_{510}) and mercury ion concentration was also provided for real-world sample detection in Figure 8b.

■ CONCLUSIONS

We have demonstrated a novel hydrophilic semi-IPN fluorescent polyHEAA hydrogel chemosensors for mercury

ion detection, which are fabricated by UV polymerization in situ-interpenetrating fluorescent polymer PA-NDBCB in polyHEAA network. Due to the strong hydrogen bond interaction between hydrophilic fluorescent polymer and polyHEAA matrix comprising distinct semi-IPN structure, tensile strength, breaking elongation of this fluorescent hydrogel can be greatly improved. Moreover, the design of hydrogel chemosensors relies on the high-efficient cyclization between Hg(II) ions and the thiourea groups that induce visible fluorescence emission change ("Green-to-Blue"). By establishing intrinsic hierarchical hydrophilic porous structures, these hydrogel chemosensors achieve ultrafast sensitive, selective mercury ion detection accompanied by the detection limit of 0.067 μM and enable facile ratiometric detection in real-world aqueous system. Notably, they work effectively even under long-term coculture in *E. coli* bacteria-laden environment. We believe that this novel strategy could inspire the future construction of soft fluorescent apparatus for hazardous Hg(II) detection in a complex real-world system.

ASSOCIATED CONTENT

Ⓢ Supporting Information

The Supporting Information is available free of charge on the ACS Publications website at DOI: 10.1021/acsabm.8b00761.

> Hg(II) stimuli-responsive mechanism, water contact angle, DSC curve and FTIR-ATR spectrum of PA-NDBCB polymer, synthetic formula of semi-IPN fluorescent hydrogels, swelling behavior of FH-3 and FH-9, performance comparison of Hg(II) detection limit with the literature, etc. (PDF)

AUTHOR INFORMATION

Corresponding Authors
*Email: luwei@nimte.ac.cn (W. L.).
*Email: tao.chen@nimte.ac.cn (T. C.).
*yangjt@zjut.edu.cn (J. Y.).

ORCID ⬚
Wei Lu: 0000-0002-2803-9519
Tao Chen: 0000-0001-9704-9545
Jintao Yang: 0000-0002-3133-1246

Notes
The authors declare no competing financial interest.

ACKNOWLEDGMENTS

REFERENCES

(1) Martin-Yerga, D.; Gonzalez-Garcia, M. B.; Costa-Garcia, A. Electrochemical Determination of Mercury: A Review. *Talanta* 2013, 116, 1091−1104.

(2) Maya, R. J.; Krishna, A.; Sirajunnisa, P.; Suresh, C. H.; Varma, R. L. Lower Rim-Modified Calix[4]arene-Bentonite Hybrid System as a Green, Reversible, and Selective Colorimetric Sensor for Hg^{2+} Recognition. *ACS Sustainable Chem. Eng.* 2017, 5 (8), 6969−6977.

(3) Bozkurt, E.; Gul, H. I. A Novel Pyrazoline-Based Fluorometric "Turn-Off" Sensing for Hg^{2+}. *Sens. Actuators, B* 2018, 255, 814−825.

(4) Tan, S. S.; Kim, S. J.; Kool, E. T. Differentiating Between Fluorescence-Quenching Metal Ions with Polyfluorophore Sensors Built on a DNA Backbone. *J. Am. Chem. Soc.* 2011, 133 (8), 2664−2671.

(5) McNutt, M. Mercury and Health. *Science* 2013, 341 (6153), 1430.

(6) Friedrich, M. J. High Mercury Levels Found in Women Around the World. *J. Am. Med. Assoc.* 2017, 318, 1857.

(7) Chen, B.; Ma, J.; Yang, T.; Chen, L.; Gao, P. F.; Huang, C. Z. A Portable RGB Sensing Gadget for Sensitive Detection of Hg^{2+} Using Cysteamine-capped QDs as Fluorescence Probe. *Biosens. Bioelectron.* 2017, 98, 36−40.

(8) Freeman, R.; Finder, T.; Willner, I. Multiplexed Analysis of Hg^{2+} and Ag$^+$ Ions by Nucleic Acid Functionalized CdSe/ZnS Quantum Dots and Their Use for Logic Gate Operations. *Angew. Chem., Int. Ed.* 2009, 48 (42), 7818−7821.

(9) Lee, J. S.; Han, M. S.; Mirkin, C. A. Colorimetric Detection of Mercuric Ion (Hg^{2+}) in Aqueous Media using DNA-functionalized Gold Nanoparticles. *Angew. Chem.* 2007, 119 (22), 4171−4174.

(10) Nolan, E. M.; Lippard, S. J. Turn-On and Ratiometric Mercury Sensing in Water with a Red-Emitting Probe. *J. Am. Chem. Soc.* 2007, 129 (18), 5910−5918.

(11) Lee, J. H.; Wang, Z.; Liu, J.; Lu, Y. Highly Sensitive and Selective Colorimetric Sensors for Uranyl (UO$_2^{2+}$): Development and Comparison of Labeled and Label-Free DNAzyme-Gold Nanoparticle Systems. *J. Am. Chem. Soc.* 2008, 130 (43), 14217−14226.

(12) Liang, F. C.; Kuo, C. C.; Chen, B. Y.; Cho, C. J.; Hung, C. C.; Chen, W. C.; Borsali, R. RGB-Switchable Porous Electrospun Nanofiber Chemoprobe-Filter Prepared from Multifunctional Co-polymers for Versatile Sensing of pH and Heavy Metals. *ACS Appl. Mater. Interfaces* 2017, 9 (19), 16381−16396.

(13) Park, H.; Kim, D. S.; Hong, S. Y.; Kim, C.; Yun, J. Y.; Oh, S. Y.; Jin, S. W.; Jeong, Y. R.; Kim, G. T.; Ha, J. S. A Skin-integrated Transparent and Stretchable Strain Sensor with Interactive Color-changing Electrochromic Displays. *Nanoscale* 2017, 9 (22), 7631−7640.

(14) Kim, S. K.; Gupta, M.; Lee, H.-i. A Recyclable Polymeric Film for the Consecutive Colorimetric Detection of Cysteine and Mercury Ions in the Aqueous Solution. *Sens. Actuators, B* 2018, 257, 728−733.

(15) Yang, J.S.; Swager, T. M. Porous Shape Persistent Fluorescent Polymer Films: An Approach to TNT Sensory Materials. *J. Am. Chem. Soc.* 1998, 120, 5321−5322.

(16) Yang, J.-Y.; Swager, T. M. Fluorescent Porous Polymer Films as TNT Chemosensors: Electronic and Structural Effects. *J. Am. Chem. Soc.* 1998, 120, 11864−11873.

(17) Lu, W.; Zhang, J.; Huang, Y.; Theato, P.; Huang, Q.; Chen, T. Self-Diffusion Driven Ultrafast Detection of ppm-Level Nitroaromatic Pollutants in Aqueous Media Using a Hydrophilic Fluorescent Paper Sensor. *ACS Appl. Mater. Interfaces* 2017, 9 (28), 23884−23893.

(18) Chen, L.; Yao, X.; Gu, Z.; Zheng, K.; Zhao, C.; Lei, W.; Rong, Q.; Lin, L.; Wang, J.; Jiang, L.; Liu, M. Covalent Tethering of Photo-responsive Superficial Layers on Hydrogel Surfaces for Photo-controlled Release. *Chem. Sci.* 2017, 8 (3), 2010−2016.

(19) Chen, Q.; Zhu, L.; Zhao, C.; Wang, Q.; Zheng, J. A Robust, One-pot Synthesis of Highly Mechanical and Recoverable Double Network Hydrogels Using Thermoreversible Sol-gel Polysaccharide. *Adv. Mater.* 2013, 25 (30), 4171−4176.

(20) Takahashi, R.; Wu, Z. L.; Arifuzzaman, M.; Nonoyama, T.; Nakajima, T.; Kurokawa, T.; Gong, J. P. Control Superstructure of Rigid Polyelectrolytes in Oppositely Charged Hydrogels via Programmed Internal Stress. *Nat. Commun.* 2014, 5, 4490−4497.

(21) Zhang, Y.; Liao, J.; Wang, T.; Sun, W.; Tong, Z. Polyampholyte Hydrogels with pH Modulated Shape Memory and Spontaneous Actuation. *Adv. Funct. Mater.* 2018, 28, 1707245.

(22) Xiao, S. W.; Yang, Y.; Zhong, M. Q.; Chen, H.; Zhang, Y. X.; Yang, J. T.; Zheng, J. Salt-Responsive Bilayer Hydrogels with Pseudo-Double-Network Structure Actuated by Polyelectrolyte and Anti-polyelectrolyte Effects. *ACS Appl. Mater. Interfaces* **2017**, *9* (24), 20843−20851.

(23) Li, M.; Sun, X.; Zhang, N.; Wang, W.; Yang, Y.; Jia, H.; Liu, W. NIR-Activated Polydopamine-Coated Carrier-Free ″Nanobomb″ for In Situ On-Demand Drug Release. *Adv. Sci.* **2018**, *5* (7), 1800155.

(24) Kim, Y. S.; Liu, M.; Ishida, Y.; Ebina, Y.; Osada, M.; Sasaki, T.; Hikima, T.; Takata, M.; Aida, T. Thermoresponsive Actuation Enabled by Permittivity Switching in An Electrostatically Anisotropic Hydrogel. *Nat. Mater.* **2015**, *14* (10), 1002−1007.

(25) Lu, W.; Ma, C.; Zhang, D.; Le, X.; Zhang, J.; Huang, Y.; Huang, C.-F.; Chen, T. Real-Time in Situ Investigation of Supramolecular Shape Memory Process by Fluorescence Switching. *J. Phys. Chem. C* **2018**, *122* (17), 9499−9506.

(26) Naficy, S.; Oveissi, F.; Patrick, B.; Schindeler, A.; Dehghani, F. Printed, Flexible pH Sensor Hydrogels for Wet Environments. *Adv. Mater. Technol.* **2018**, *3*, 1800137.

(27) Lu, W.; Le, X.; Zhang, J.; Huang, Y.; Chen, T. Supramolecular Shape Memory Hydrogels: A New Bridge Between Stimuli-Responsive Polymers and Supramolecular Chemistry. *Chem. Soc. Rev.* **2017**, *46* (5), 1284−1294.

(28) Dai, X.; Zhang, Y.; Gao, L.; Bai, T.; Wang, W.; Cui, Y.; Liu, W. A Mechanically Strong, Highly Stable, Thermoplastic, and Self-Healable Supramolecular Polymer Hydrogel. *Adv. Mater.* **2015**, *27* (23), 3566−3571.

(29) Tang, L.; Liu, W.; Liu, G. High-strength Hydrogels with Integrated Functions of H-Bonding and Thermoresponsive Surface-Mediated Reverse Transfection and Cell Detachment. *Adv. Mater.* **2010**, *22* (24), 2652−2656.

(30) Choi, S.; Kim, J. Designed Fabrication of Super-Stiff, Anisotropic Hybrid Hydrogels via Linear Remodeling of Polymer Networks and Subsequent Crosslinking. *J. Mater. Chem. B* **2015**, *3* (8), 1479−1483.

(31) Zhao, Y.; Li, M.; Liu, B.; Xiang, J.; Cui, Z.; Qu, X.; Qiu, D.; Tian, Y.; Yang, Z. Ultra-tough Injectable Cytocompatible Hydrogel for 3D Cell Culture and Cartilage Repair. *J. Mater. Chem. B* **2018**, *6* (9), 1351−1358.

(32) Zhang, D.; Zhang, Y.; Lu, W.; Le, X.; Li, P.; Huang, L.; Zhang, J.; Yang, J.; Serpe, M. J.; Chen, D.; Chen, T. Fluorescent Hydrogel-coated Paper/Textile as Flexible Chemosensor for Visual and Wearable Mercury(II) Detection. *Adv. Mater. Technol.* **2019**, *4*, 1800201.

(33) Hung, H. C.; Jain, P.; Zhang, P.; Sun, F.; Sinclair, A.; Bai, T.; Li, B.; Wu, K.; Tsao, C.; Liu, E. J.; Sundaram, H. S.; Lin, X.; Farahani, P.; Fujihara, T.; Jiang, S. A Coating-free Nonfouling Polymeric Elastomer. *Adv. Mater.* **2017**, *29* (31), 1700617.

(34) Zhou, X.; Zhao, F.; Guo, Y.; Zhang, Y.; Yu, G. A Hydrogel-based Antifouling Solar Evaporator for Highly Efficient Water Desalination. *Energy Environ. Sci.* **2018**, *11*, 1985−1992.

(35) Zhao, C.; Chen, Q.; Patel, K.; Li, L.; Li, X.; Wang, Q.; Zhang, G.; Zheng, J. Synthesis and Characterization of pH-Sensitive Poly(N-2-Hydroxyethyl-acrylamide)-acrylic Acid (Poly(HEAA/AA)) Nano-gels with Antifouling Protection for Controlled Release. *Soft Matter* **2012**, *8* (30), 7848.

(36) Zhang, D.; Fu, Y.; Huang, L.; Zhang, Y.; Ren, B.; Zhong, M.; Yang, J.; Zheng, J. Integration of Antifouling and Antibacterial Properties in Salt-Responsive Hydrogels with Surface Regeneration Capacity. *J. Mater. Chem. B* **2018**, *6* (6), 950−960.

(37) Zhang, J.; Xiao, S.; Shen, M.; Sun, L.; Chen, F.; Fan, P.; Zhong, M.; Yang, J. Aqueous Lubrication of Poly(N-Hydroxyethyl Acryl-amide) Brushes: A Strategy for Their Enhanced Load Bearing Capacity and Wear Resistance. *RSC Adv.* **2016**, *6* (26), 21961−21968.

(38) Zheng, S. Y.; Ding, H.; Qian, J.; Yin, J.; Wu, Z. L.; Song, Y.; Zheng, Q. Metal-Coordination Complexes Mediated Physical Hydro-gels with High Toughness, Stick−Slip Tearing Behavior, and Good Processability. *Macromolecules* **2016**, *49* (24), 9637−9646.

(39) Wu, B.; Zhang, L.; Huang, L.; Xiao, S.; Yang, Y.; Zhong, M.; Yang, J. Salt-Induced Regenerative Surface for Bacteria Killing and Release. *Langmuir* **2017**, *33* (28), 7160−7168.

(40) Huang, L.; Zhang, L.; Xiao, S.; Yang, Y.; Chen, F.; Fan, P.; Zhao, Z.; Zhong, M.; Yang, J. Bacteria Killing and Release of Salt-Responsive, Regenerative, Double-Layered Polyzwitterionic Brushes. *Chem. Eng. J.* **2018**, *333*, 1−10.

(41) Dubinov, A. E.; Kitaev, I. N. Generalized Wien's Displacement Law and Stefan-Boltzmann Law for Thermal Radiation with A Nonzero Chemical Potential. *J. Opt. Technol.* **2018**, *85* (6), 314−316.

(42) Zhang, H.; Gao, X.; Chen, K.; Li, H.; Peng, L. Thermo-sensitive and Swelling Properties of Cellouronic Acid Sodium/Poly (Acryl-amide-co-Diallyldimethylammonium Chloride) Semi-IPN. *Carbohydr. Polym.* **2018**, *181*, 450−459.

(43) Liu, Y.; Zhang, K.; Ma, J.; Vancso, G. J. Thermoresponsive Semi-IPN Hydrogel Microfibers from Continuous Fluidic Processing with High Elasticity and Fast Actuation. *ACS Appl. Mater. Interfaces* **2017**, *9* (1), 901−908.

(44) Jeon, O.; Shin, J.-Y.; Marks, R.; Hopkins, M.; Kim, T.-H.; Park, H.-H.; Alsberg, E. Highly Elastic and Tough Interpenetrating Polymer Network-Structured Hybrid Hydrogels for Cyclic Mechanical Loading-enhanced Tissue Engineering. *Chem. Mater.* **2017**, *29* (19), 8425−8432.

(45) Zhu, B.; Gao, C.; Zhao, Y.; Liu, C.; Li, Y.; Wei, Q.; Ma, Z.; Du, B.; Zhang, X. A 4-Hydroxynaphthalimide-Derived Ratiometric Fluorescent Chemodosimeter for Imaging Palladium in Living Cells. *Chem. Commun.* **2011**, *47* (30), 8656−8658.

(46) Liu, B.; Tian, H. A Selective Fluorescent Ratiometric Chemodosimeter for Mercury Ion. *Chem. Commun.* **2005**, *47* (25), 3156−3158.

(47) Bozdemir, O. A.; Buyukcakir, O.; Selcuk, S.; Kolemen, S.; Gulseren, G.; Nalbantoglu, T.; Boyaci, H.; Akkaya, E. U. Selective Manipulation of ICT and PET Processes in Styryl-Bodipy Derivatives: Applications in Molecular Logic and Fluorescence Sensing of Metal Ions. *J. Am. Chem. Soc.* **2010**, *132* (23), 8029−8036.

(48) Song, Z.; Wang, F.; Qiang, J.; Zhang, Z.; Chen, Y.; Wang, Y.; Zhang, W.; Chen, X. Fluorescent Probe Encapsulated Hydrogel Microsphere for Selective and Reversible Detection of Hg^{2+}. *J. Lumin.* **2017**, *183*, 212−216.